Glow-Discharge Hydrogenated Amorphous Silicon, edited by K. Tanaka, pp. 227–249.

Chapter 10

JUNCTION PROPERTIES OF AMORPHOUS SEMICONDUCTORS

Hideharu MATSUURA

Electrotechnical Laboratory, 1-1-4 Umezono, Tsukuba, Ibaraki 305, Japan

10.1 Introduction

The structural and electronic properties of amorphous semiconductors are much different from those of their crystalline counterparts, as described in previous sections. Therefore, in order to understand the junction properties of amorphous semiconductors microscopically, we need new theories which can take into account the electronic features of amorphous semiconductors, instead of conventional theories for crystalline semiconductor junctions which have already been established.[1] However, many reports have explained the junction properties of amorphous semiconductors using crystalline semiconductor theories.[2–10] For example, they have tried to understand that currents in metal/amorphous semiconductor junctions are limited by thermionic emission (or diffusion) if ideal factors (η-values) are unity, and that recombination currents are dominant if η-values are larger than unity.[8,11] There is, however, such a high density of defects in amorphous films that carrier collisions in the depletion region cannot be ignored, and multistep tunneling (hopping) through the barrier may occur easily. Specifically, the assumptions which have been made in the theory of crystalline semiconductor junctions are not always valid for amorphous semiconductor junctions.

We describe the properties of contacts between amorphous semiconductors and metals (or crystalline silicon) in the next section in order to understand their rectifying properties. In sections 10.3 and 10.4, we propose models for amorphous semiconductor junctions which can explain our experimental data concerning Schottky barrier junctions as well as amorphous/crystalline heterojunctions. In section 10.5 we describe properties of a-Si:H *p-i-n* junctions. Section 10.6 summarizes this chapter.

10.2 *Properties of Contacts between Amorphous Semiconductors and Other Materials*[12,13]

Diodes with four different structures were fabricated to determine the conduction type of hydrogenated amorphous silicon (a-Si:H) films with different doping ratios of PH_3 or B_2H_6 to SiH_4, and to obtain the contact properties (ohmic or rectifying). The structures are: type-1 (Au/a-Si:H/n^+ c-Si), type-2 (Au/a-Si:H/p^+ c-Si), type-3 (Mg/a-Si:H/n^+ c-Si), and type-4 (Mg/a-Si:H/p^+ c-Si).

In the case of undoped a-Si:H, shown in Fig. 10.1(a), the type-3 diode shows ohmic behavior and the current is limited by the resistance of the a-Si:H film, which means that both contacts of Mg/a-Si:H and n^+ c-Si/a-Si:H are ohmic. Currents of type-2 and type-4 diodes, for a positive bias on both metals, are of the same order of magnitude as each other, indicating that those currents are limited by a reverse-bias p^+ c-Si/a-Si:H junction in both diodes. Likewise, the similarity between the J-V characteristics of type-1 and type-2 diodes for a negative bias on the metal (Au) implies that the

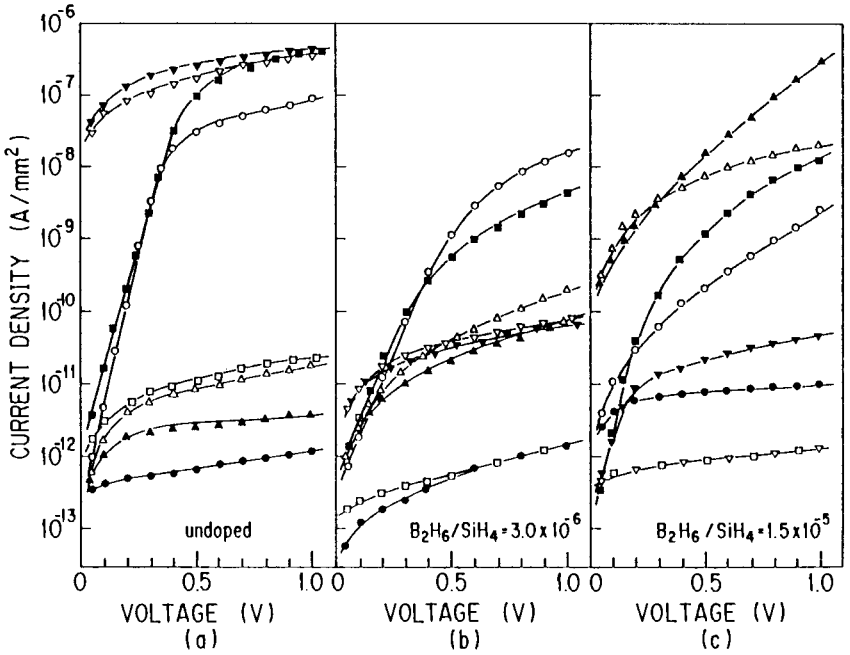

Fig. 10.1. Current density-voltage characteristics of four different types of diodes: ○●, type-1; △▲, type-2; ▽▼, type-3; and □■, type-4. Open and solid marks represent data points for a positive bias and a negative bias on the metal, respectively (after Matsuura *et al.*[13]).

currents are limited by a reverse-bias Au/a-Si:H junction. The properties of the junctions involved in each diode for undoped films can then be classified qualitatively into 'R' (rectifying) or 'O' (ohmic), summarized in the first row of Table 10.1.

Since the contact properties of undoped a-Si:H are similar to those of phosphorus (P)-doped a-Si:H, the conduction of undoped a-Si:H is of the n-type. From a similar experiment, moreover, Mg is found to form an ohmic contact with undoped and P-doped hydrogenated amorphous silicon-germanuim alloys (a-$Si_{1-x}Ge_x$:H).[14]

Diodes of B-doped a-Si:H with B_2H_6/SiH_4 ratios of 7.0×10^{-7}, 1.5×10^{-6}, and 3.0×10^{-6} all exhibit similar characteristics shown in Fig. 10.1(b). The forward currents of type-1 and type-4 diodes at higher voltages are limited by the resistance of the B-doped a-Si:H film. Since the currents of type-2 and type-3 diodes are substantially lower than the forward currents of type-1 and type-4 diodes at higher voltages, it is reasonable to consider type-2 and type-3 diodes as back-to-back diodes. Then all junctions of Au/a-Si:H, Mg/a-Si:H, p^+ c-Si/a-Si:H, and n^+ c-Si/a-Si:H are rectifying, as shown in Table 10.1. The conduction type of B-doped a-Si:H with $B_2H_6/SiH_4\sim10^{-6}$ is intrinsic.

From similar analysis of the J-V characteristics of $B_2H_6/SiH_4=1.5\times10^{-5}$ shown in Fig. 10.1(c), all of the diode junctions have been designated as 'O' or 'R', and are summarized in Table 10.1. The conduction of B-doped a-Si:H with $B_2H_6/SiH_4>10^{-5}$ is of the p-type.

This study is important for understanding where diode currents are limited (i.e., in a junction or in the bulk) and also which contact exhibits a rectifying property. For example, Šmíd *et al.*[15] considered that the forward currents of Mg/undoped a-Si:H/p c-Si heterojunctions at 0.1 V$<V<$0.5 V were space-charge-limited currents (bulk-limited currents) because the current was proportional to forward voltages lower than 0.1 V, and then increased rapidly with V. Per the discussion of contact properties, however, the forward current is limited by the a-Si:H/p c-Si heterojunction, as

Table 10.1. Properties of contacts with a-Si:H.

	Au	p^+ c-Si	Mg	n^+ c-Si	conduction type[b]
P-doped and undoped	R	R	O	O	*n*
$B_2H_6/SiH_4\sim10^{-6}$	R	R	R	R	intrinsic
$B_2H_6/SiH_4>10^{-5}$	O	O	R	R	*p*

[a]R: rectification, O: ohmic.
[b]Based on 'dominant carrier concentration' (present study).

expressed by $J \propto \exp(AV)-1$. The current is proportional to V lower than 0.1 V because $\exp(AV)$ can approximately expand $1+AV$ in Talor's series at $V<0.1$ V. This current is, however, not an ohmic current as Šmíd *et al.* insisted it was.

10.3 Amorphous Schottky Barrier Junctions[14,16]

10.3.1 Theoretical analysis

According to the thermionic-emission theory for crystalline semiconductors,[17] the shape of the barrier profile is immaterial and the current flow depends solely on the barrier height, since it is assumed that electron collisions in the depletion region can be neglected. The various ways in which electrons can be transported across the Schottky barrier junction under forward bias are shown schematically for an n-type crystalline semiconductor in Fig. 10.2(a). The mechanisms are as follows:

(a) the emission of electrons from the semiconductor over the top of the barrier into the metal (the thermionic-emission current J_T);

(b) quantum-mechanical tunneling through a part of the barrier (the thermionic-field-emission current J_{TF});

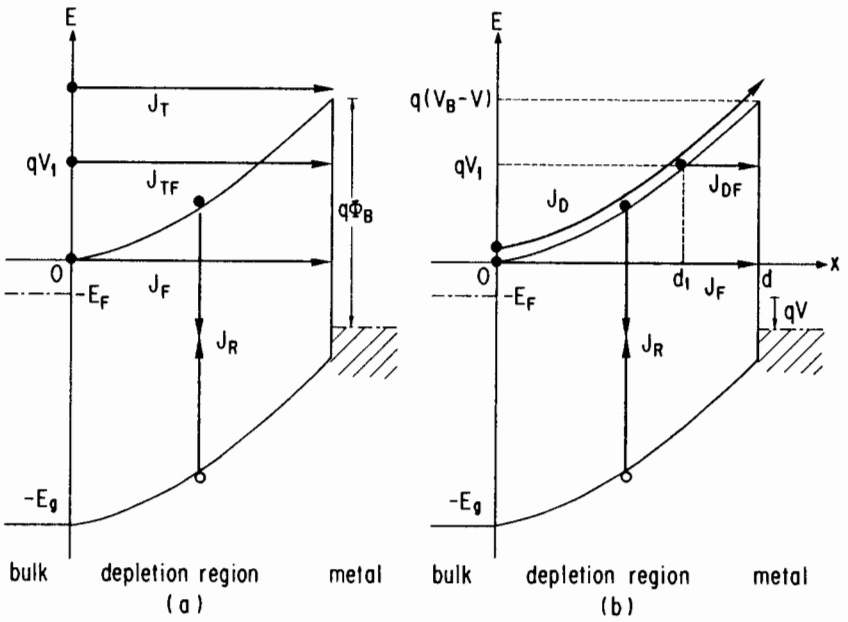

Fig. 10.2. Energy-band diagrams for Schottky barrier semiconductor junctions with definitions of symbols defined in the text. The various current paths, (a) in crystalline and (b) in amorphous semiconductors, are also indicated (after Matsuura and Okushi[14]).

(c) quantum-mechanical tunneling through the barrier from the edge of the depletion region (the field-emission current J_F);

(d) recombination in the depletion region (the recombination current J_R).

It is possible to make practical Shottky barrier diodes in which (a) is the most important; these diodes are generally referred to as being nearly ideal. Processes (b), (c), and (d) cause departures from this ideal behavior. Processes (b) and (c) appear only in the case of degenerated semiconductors at low temperatures.[18]

In amorphous semiconductors, on the other hand, electron collisions in the depletion region cannot be neglected because of the existence of many defects. This means that the diffusion current J_D of Fig. 10.2(b) is more important to amorphous Schottky barrier junctions than J_T (Fig. 10.2(a)). In actual amorphous Schottky barrier junctions, besides the diffusion current (J_D), the recombination current (J_R) and the tunneling currents (J_{DF} and J_F), due to multistep tunneling via localized states in the depletion region, flow across the Schottky barrier as shown in Fig. 10.2(b). In nondegenerated crystalline semiconductors, J_{DF} in Fig. 10.2(b) is not taken into account in the current transport, because tunneling via localized states in the depletion region can be neglected. J_{DF} is a concept peculiar to amorphous semiconductor junctions (here, J_{DF} is the diffusion-field-emission current) and is considered as follows.

The tunneling current at $E=qV_1$ (or $x=d_1$) is proportional to the product of the density of electrons near the conduction band edge at $x=d_1$ and the tunneling probability from $x=d_1$ to d. Assuming that the maximum of the tunneling currents in the energy range of 0 eV$<E<q(V_B-V)$ eV is close to J_{DF},

$$J_{DF} \propto \exp(V/E_0), \tag{1}$$

with

$$E_0 = E_{00}\coth(qE_{00}/kT) \tag{2}$$

and

$$E_{00} = [(1+\gamma)h/4\pi](N_I/m^*\varepsilon_s)^{1/2} \tag{3}$$

where γ is the multistep tunneling factor and $\gamma=0$ when the one-step tunneling process is dominant, N_I is the effective density of the donor-like states, k the Boltzmann constant, T the measuring temperature, h Planck's constant, m^* the effective mass of electrons, and ε_s the semiconductor permittivity.

This diffusion-field-emission current J_{DF} must be a current peculiar to amorphous Schottky barrier junctions. Currents J_F and J_D can be considered special cases of J_{DF}.

In one case ($d_1=0$) where electrons tunnel through the whole Schottky barrier, this current is the field-emission current and can be derived as

$$J_F \propto \exp(V/E_{00}). \tag{4}$$

The slope ($1/E_{00}$) of the $\ln(J)$-V relation does not depend on the temperature, as is clear from Eqs. (3) and (4).

In the other case ($d_1=d$) where all electrons are diffused over the entire depletion region, this current is called the diffusion current and can be described as[17]

$$J_D \propto qN_C\mu F\exp(-q\phi_B/kT)\exp(qV/kT), \tag{5}$$

where F is the electric field in the semiconductor near the metal-semiconductor interface, $q\phi_B$ the barrier height of qV_B plus E_F, and μ the electron mobility. Since the electric field F varies with V, Eq. (5) can be rewritten as

$$J_D \propto \exp(qV/\eta kT), \tag{6}$$

where $\eta=1.06$ (Ref. 11). The diffusion current J_D is a desirable current in amorphous Schottky barrier junctions.

The diffusion-field-emission current is dominant in most amorphous Schottky barrier junctions. When the density of gap states is considerably high, the forward current becomes the field-emission current. On the other hand, when it is fairly low, it becomes the diffusion current.

10.3.2 Comparison to experimental results

The Schottky barrier junctions consisted of amorphous materials (a-Si:H or a-$Si_{1-x}Ge_x$:H) and gold (Au) as follows; undoped a-Si:H (diode-A), 905-ppm P-doped a-$Si_{1-x}Ge_x$:H deposited by a triode reactor chamber (diode-B), 7.8-ppm and 1080-ppm P-doped a-$Si_{1-x}Ge_x$:H deposited by a triode reactor chamber using H_2-diluted starting-gas materials (diodes C1 and C2, respectively). The optical gaps of all a-$Si_{1-x}Ge_x$:H used in this study were kept at 1.5 eV.

The thickness dependence of the forward currents of undoped a-Si:H diodes was investigated. The forward current is inversely proportional to the thickness of a-Si:H according to the diffusion theory, while it is kept constant according to the thermionic-emission theory. It is experimentally found that the forward current is inversely proportional to the thickness of a-Si:H at 361 K where the η-value of the diode of each thickness is close to

1.1 (Ref. 19). Therefore, our undoped a-Si:H Schottky barrier diode is limited by the diffusion J_D.

The temperature dependence of the slope of the $\ln(J)$-V curve in a-$Si_{1-x}Ge_x$:H diodes at forward voltages was studied. Since the slope of diode-B does not vary with the temperature, the field-emission current is dominant in diode-B according to Eq. (4). The forward currents of diodes C1 and C2 are limited by the diffusion-field-emission because these follow Eq. (1), as shown in Fig. 10.3.

From the investigations of spin densities obtained from electron spin resonance (ESR) and ratios of photoconductivity to dark conductivity, the qualities of the a-$Si_{1-x}Ge_x$:H films deposited by the triode reactor chamber using H_2-diluted starting-gas materials are found to be better than those deposited by only the triode reactor chamber. Moreover, the qualities of the a-Si:H films are found to be best. Corresponding to the film qualities, the forward current of diode-A is a diffusion current, which is a desirable current in amorphous Schottky barrier junctions; the currents of diodes C1 and C2 are diffusion-field-emission currents, and the current of diode B is a field-emission current. Moreover, diodes which consist of a-$Si_{1-x}Ge_x$:H films deposited by a diode reactor chamber, whose qualities are worse than the other materials mentioned above, do not exhibit a rectifying property.

The values of E_{00} obtained from their J-V characteristics were 3.1×10^{-2}, 1.7×10^{-2}, and 2.3×10^{-2} eV for diodes B, C1 and C2, respectively. However,

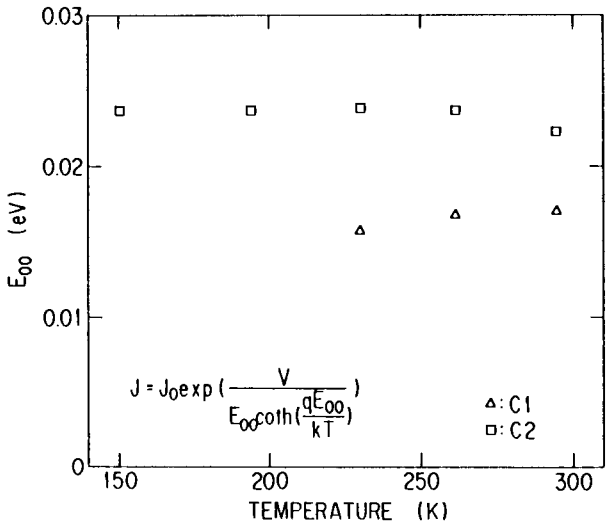

Fig. 10.3. Temperature dependence of E_{00} estimated from Eq. (2). Those values for diodes C1 and C2 are independent of temperature (after Matsuura and Okushi[14]).

E_{00} can independently be estimated by Eq. (3) using the experimental values of N_I. Since N_I of diodes B, C1 and C2 were obtained from their $1/C^2$-V relationships as 1.4×10^{17}, 2.4×10^{16}, and 1.5×10^{17} cm^{-3}, respectively, E_{00} were estimated to be 1.8×10^{-3}, 7.2×10^{-4}, and 1.8×10^{-3} eV, respectively, if one-step tunneling ($\gamma=0$) was assumed. In this estimation, $\varepsilon_s=16\varepsilon_0$ and $m^*=m_0$ were used, where ε_0 is the free-space permittivity and m_0 the free-electron mass. The above values are much smaller than those obtained fom the J-V characteristics. This estimation gap does essentially exist even when $m^*=0.1m_0$ is used, suggesting that the assumption of one-step tunneling in Eq. (3) is wrong. Consequently, it is reasonable to consider that multistep tunneling ($\gamma>0$) is dominant in amorphous Schottky barrier junctions.

10.4 Amorphous/Crystalline Heterojunctions[20-22]

10.4.1 Capacitance-voltage characteristics

The depletion region formed by an undoped a-Si:H/p-type c-Si heterojunction is considered. When a reverse *dc* voltage (V_{DC}) is applied, it produces space-charge layers both in a-Si:H and c-Si. Under the assumption that this p c-Si has only shallow acceptors, the space charge in the p c-Si is formed by negatively-charged acceptors. However, a-Si:H possesses gap states. The origin of the space charge in a-Si:H is schematically discussed. In the neutral region, all the gap states below the Fermi level (E_F) are occupied by electrons, while in the depletion region the gap states above E_{OB2}, as indicated by the hatched area in Fig. 10.4(a), are vacant of electrons, where E_{OB2} is determined from the condition that the thermal-emission rate for electrons is equal to that for holes, and given by

$$E_{OB2} = E_V + E_{g2}/2 + (kT/2)\ln(\nu_p/\nu_n) \tag{7}$$

where ν_p and ν_n are the attempt-to-escape frequencies for holes and electrons, respectively.[23] Therefore, the gap states in the hatched area in Fig. 10.4(a) behave like positive space charges, here referred to as donor-like states, and the density of the donor-like states is constant between spatial position 0 and W_2. This, together with the density of donors (if they exist), gives the effective density of the donor-like states (N_I) , as shown in Fig. 10.4(c). Figure 10.4(b) shows the potential variation with distance where V_B is the built-in voltage. The depletion widths (W_1 and W_2) are given by

$$qN_AW_1 \simeq qN_IW_2, \tag{8}$$

$$W_1 = [2\varepsilon_{s1}(V_{B1} - V_{DC1})/qN_A]^{1/2}, \tag{9}$$

and

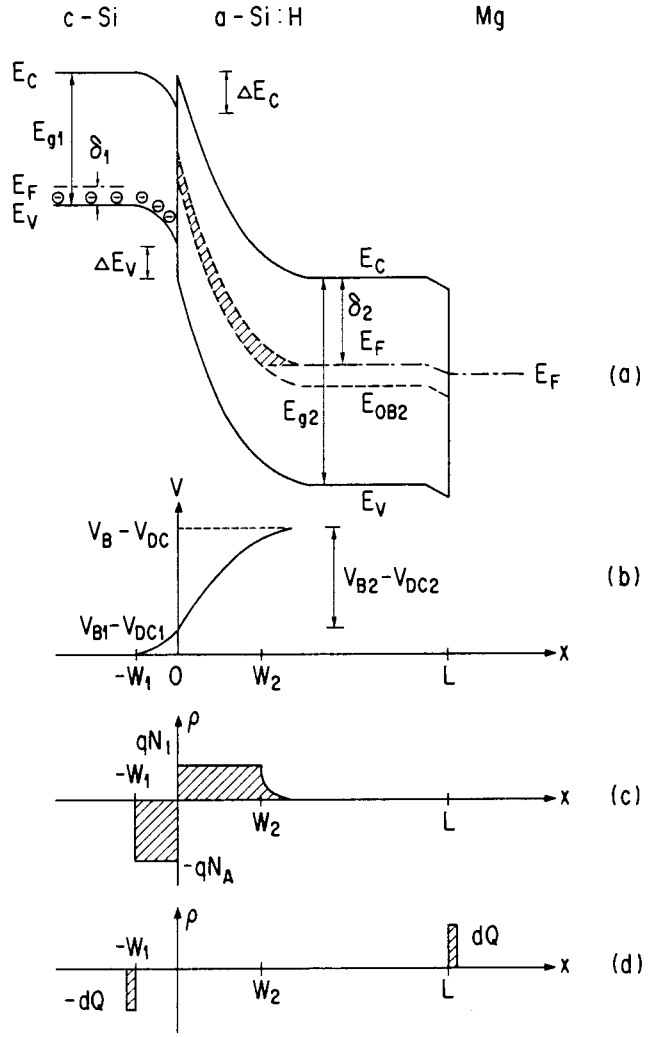

Fig. 10.4. Schematic sketches of the heterojunction: (a) energy-band diagram; (b) potential variation; (c) space-charge density for a reverse *dc* voltage; (d) charge density for a small *ac* voltage (after Matsuura[55]).

$$W_2 \simeq [2\varepsilon_{s2}(V_{B2} - V_{DC2})/qN_I]^{1/2}. \tag{10}$$

Here N_A is the density of the acceptors in the p c-Si and ε_s the semiconductor permittivity. In Fig. 10.4, δ indicates the distance in energy from the Fermi level to the nearest band edge, E_g the energy band gap of the semiconductor,

W the width of the depletion region, L the thickness of a-Si:H, and ΔE the difference in energy between band edges of the two semiconductors. The subscripts 1 and 2 refer to p c-Si and undoped a-Si:H, respectively, and the subscripts C and V refer to the conduction band and the valence band, respectively.

The capacitance of the heterojunction was measured using a small *ac* voltage at 100 kHz. The resistivity (ρ_1) of p c-Si used in this study is lower than 10 Ωcm so that the dielectric relaxation time ($\varepsilon_{s1}\rho_1$) becomes 10^{-11} sec, indicating that the capacitance (C_1) in c-Si is given by

$$C_1 = \varepsilon_{s1}/W_1. \tag{11}$$

On the other hand, the resistivity (ρ_2) of undoped a-Si:H used is about 10^9 Ωcm. In this case the dielectric relaxation time becomes 10^{-3} sec, suggesting that the undoped a-Si:H film may be considered a dielectric material in its behavior in the case of the 100-kHz *ac* voltage; then the capacitance (C_2) in a-Si:H should be given by

$$C_2 = \varepsilon_{s2}/L. \tag{12}$$

The measured capacitance (C) at 100 kHz is from series of C_1 and C_2, and is expressed as

$$1/C = 1/C_1 + 1/C_2, \tag{13}$$

because spatially the redistribution of charge can respond to the 100-kHz *ac* voltage at W_1 and L, as shown in Fig. 10.4(d). From Eqs. (8)–(10), the following equation is obtained:

$$(V_{B1} - V_{DC1})/(V_{B2} - V_{DC2}) \simeq N_1\varepsilon_{s2}/N_A\varepsilon_{s1}. \tag{14}$$

The final equation is obtained as

$$\begin{aligned} W_1^2 &= [\varepsilon_{s1}(1/C - 1/C_2)]^2 \\ &\simeq 2\varepsilon_{s1}\varepsilon_{s2}N_1(V_B - V_{DC})/qN_A(N_A\varepsilon_{s1} + N_1\varepsilon_{s2}) \end{aligned} \tag{15}$$

from Eqs. (9), (11), (13), and (14).

Figure 10.5 shows the W_1^2 vs. V_{DC} relationship and the data reveal a good linear relationship, indicating that the heterojunction model mentioned is applicable to the present system. As is clear from Eq. (15), magnitudes of N_1 and V_B can be graphically determined from the slope and the intercept on the abscissa, respectively.

The electron affinity (χ_2) of a-Si:H can be determined from C-V

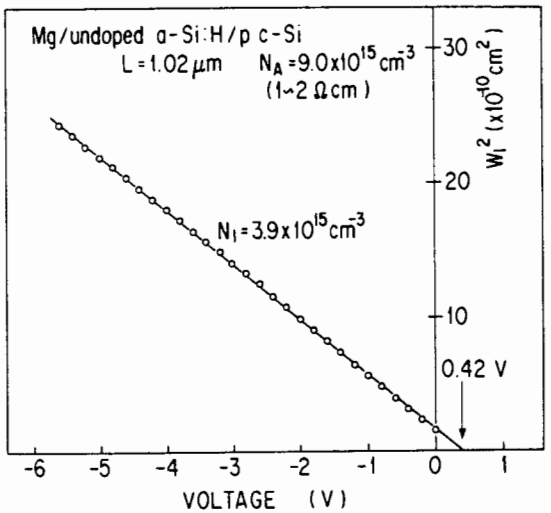

Fig. 10.5. Width of the depletion region in c-Si as a function of *dc* voltage (after Matsuura *et al.*[20]).

characteristics of those heterojunctions. As is clear from the energy band diagram shown in Fig. 10.4(a), ΔE_C is expressed by

$$\Delta E_C = \delta_1 + \delta_2 - E_{g1} + qV_B, \tag{16}$$

as well as

$$\Delta E_C = \chi_1 - \chi_2. \tag{17}$$

By substituting quantitative data on δ_1, δ_2, χ_1, E_{g1}, and V_B to Eqs. (16) and (17), ΔE_C and χ_2 were determined as

$$\Delta E_C = 0.20 \pm 0.07 \text{ eV}$$

and

$$\chi_2 = 3.85 \pm 0.07 \text{ eV}$$

using E_{g1}=1.12 eV and χ_1=4.05 eV (Ref. 24). Figure 10.6 shows the energy band diagrams for each diode with different p c-Si resistivities, sketched on the basis of the above results.

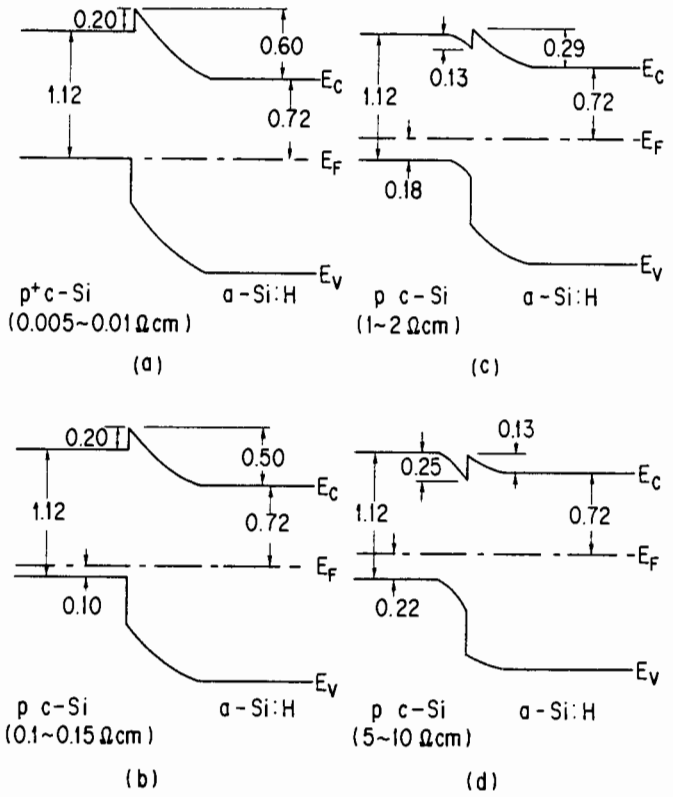

Fig. 10.6. Energy-band diagrams in the junction region for heterojunctions using c-Si with four different resistivities (after Matsuura *et al.*[21]).

10.4.2 Current-voltage characteristics

J-V characteristics of the diodes with the following four different resistivities of *p* c-Si in Fig. 10.6 have been measured as a function of temperature in the range between 297 and 374 K: 0.005~0.01-Ωcm *p* c-Si (sample 1), 0.1~0.15-Ωcm *p* c-Si (sample 2), 1~2-Ωcm *p* c-Si (sample 3), and 5~10-Ωcm *p* c-Si (sample 4). Figure 10.7 shows the *J-V* characteristics of sample 1 and its temperature dependence. In all samples, linear relationships between log(*J*) and *V* at forward voltages lower than 0.5 V were clearly observed at each temperature.

According to either of the diffusion models, the thermionic-emission model or the recombination model, the relation between *J* and *V* is represented by

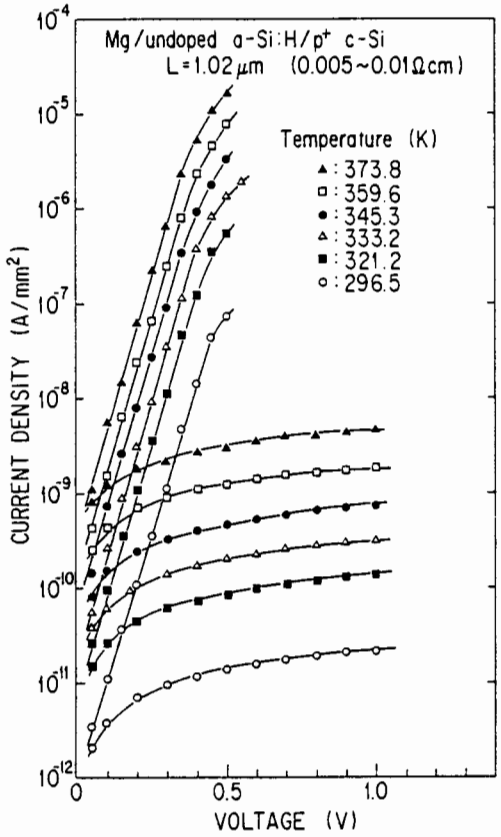

Fig. 10.7. *J-V* characteristics of sample 1 measured at six different temperatures (after Matsuura *et al.*[21]).

$$J \propto \exp(qV/\eta kT), \tag{18}$$

where k is the Boltzmann's constant, T the measuring temperature, and η the ideal factor being independent of temperature.[1]

As is clear from the results shown in the figure, the slope of the forward characteristics is kept constant for several temperatures, which indicates that Eq. (18) is not valid in the present system. The current is described as

$$J = J_0 \exp(AV), \tag{19}$$

and

$$J_0 \propto \exp(-\Delta E_{af}/kT), \tag{20}$$

where A and ΔE_{af} are temperature-independent constants. From Eq. (20), ΔE_{af} were estimated as 0.72, 0.80, 0.65, and 0.63 eV for samples 1–4, respectively. Since Eq. (19) is applicable to the present system, the forward current is limited by tunneling.

Models for junction transport based on the tunneling process, proposed by several authors,[25,26] are schematically shown in Fig. 10.8(a). To explain the present experimental results, each model is examined one by one.

The simplest tunneling model consists of the tunneling of carriers through the spike-shaped barrier in the conduction band (Fig. 10.8(a)). According to Riben *et al.*,[25] predominant tunnel flux takes place at an energy close to the peak of the barrier within an energy difference of about 0.1 eV for crystalline heterojunctions, indicated by path A in the figure. In the present heterojunction, however, the tunneling process at an energy range far below the barrier peak, indicated by path B in the figure, is quite

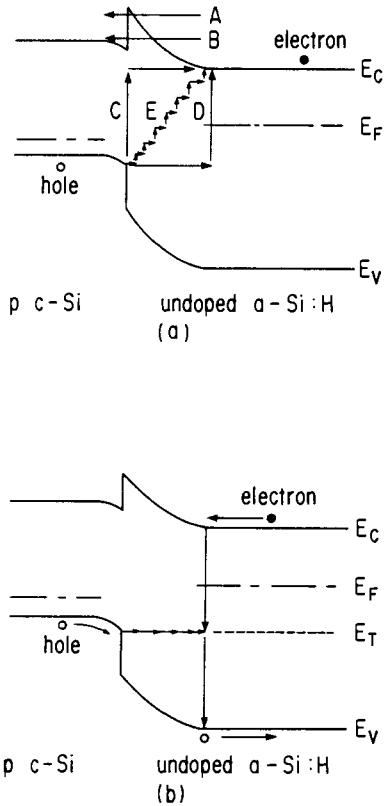

Fig. 10.8. Tunneling models for heterojunctions. (a) Reported tunneling models, (b) the multistep tunneling capture-emission model (after Matsuura *et al.*[21]).

possible because localized states are quasi-continuously distributed within the gap of a-Si:H, spatially as well as energetically. As is clear from the model, the magnitude of ΔE_{af} is expected to be larger than 1.12 eV for sample 1. This requirement contradicts the actual data, i.e., the ΔE_{af} of sample 1 was obtained experimentally as 0.72 eV.

A second model, based on the tunneling process of carriers, has originally been presented for excess current in tunnel diodes.[1] As has been discussed by Riben *et al.*,[25] tunneling current by one-step tunneling (C or D in Fig. 10.8(a)) is always smaller than that by multistep tunneling (E in the figure). If we assume that their discussion can be applied to the present a-Si:H/c-Si heterojunction, the multistep tunneling process should predominate in the present system since localized states are quasi-continuously distributed in the mobility gap. According to this multistep tunneling process, however, J_0 should change exponentially with T due to the temperature dependence of the band gap, while J_0 obtained in this study varies exponentially with $-1/T$ as shown in Eq. (20).

In order to solve this disagreement, we propose the multistep tunneling capture-emission process as the most probable model for the present system, which is shown in Fig. 10.8(b). A hole in the valence band of p c-Si flows from one localized state to another in a-Si:H located within an energy range of kT by a multistep tunneling process, and keeps flowing until the tunneling rate becomes smaller than the rate for hole release from the state to the valence band of a-Si:H, or for recombination of the hole with an electron in the conduction band of a-Si:H. The end point of the tunneling might be close to the edge of the depletion layer of a-Si:H, where the tunneling rate decreases due to a decrease of the electric field.

Thus, a current density flowing from p c-Si to undoped a-Si:H is given by

$$J = B(e_p + \sigma_n v_{th} n)\exp(AV), \tag{21}$$

where B is a constant independent of applied voltage and temperature,* e_p the hole emission rate given as $e_p = \sigma_p v_{th} N_V \exp[-(E_T - E_V)/kT]$, σ_n the capture cross section of electrons, v_{th} the thermal velocity, n the electron density in the conduction band of a-Si:H given as $n = N_C \exp[-(E_C - E_F)/kT]$, σ_p the capture cross section of holes, N_V and N_C the effective densities of states in the valence band and the condition band of a-Si:H, respectively, and E_F, E_T, E_V, and E_C the energies of the Fermi level, the localized state, the valence band, and the conduction band of a-Si:H, repectively. The current density is described as

*Although B depends on the measuring temperature due to the temperature dependence of the band gap, this temperature dependence is much smaller than those of e_p and n. Therefore, the temperature dependence of B can be neglected.

$$J = J_0 \exp(AV), \tag{22}$$

with

$$J_0 = B\{\sigma_p v_{th} N_V \exp[-(E_T - E_V)/kT] + \sigma_n v_{th} N_C \exp[-(E_C - E_F)/kT]\}. \tag{23}$$

By comparing Eqs. (22) and (23) with the experimental data, several possible comments can be deduced. For the junction property using the lowest-resistivity p c-Si (sample 1), ΔE_{af}=0.72 eV was obtained. This value coincides with that of the activation energy δ_2 ($=E_C - E_F$) of the dark conductivity of undoped a-Si:H. Therefore, considering the band diagram shown in Fig. 10.6(a), the electron capture rate is larger than the hole emission rate, i.e., the second term predominates in the right-hand side of Eq. (23). On the other hand, for samples 2–4, the obtained values of ΔE_{af} were 0.80, 0.65, and 0.63 eV, respectively, which correlates with an increase in the substrate resistivity as shown in Fig. 10.6(b)–(d). It suggests that hole emission dominantly prevails for these three samples, namely, the first term in the right-hand side of Eq. (23) determines a magnitude of J_0.

10.5 a-Si:H p-i-n Diodes[19]

Dark J-V characteristics of a-Si:H p-i-n diodes with various thicknesses of the intrinsic layer (i layer)(770–9300 Å) are systematically investigated and from those results the current transport mechanism is discussed. Three types of sample configurations are: type-A (glass/ITO/SnO_2/p-i-n/Mg); type-B (stainless steel/p-i-n/Mg); and type-C (stainless steel/p-i/Mg). Here the i-layer is undoped a-Si:H. Mg has been found to form an ohmic contact with undoped a-Si:H as well as P-doped a-Si:H, as mentioned in section 10.2.

Figure 10.9 shows the thickness dependence of the J-V characteristics of the p-i-n diodes (type-A) at room temperature. The magnitude of the forward current in the voltage range (V<0.5 V) where the current density increases exponentially with V is independent of the i layer thickness, while the thickness dependence of the J-V characteristics appears in other ranges: (1) the forward current at higher voltages (V>0.5 V) decreases with increasing i layer thickness, probably due to an increase of the bulk series resistance of the i layer, and (2) a breakdown of the reverse current appears at lower reverse bias voltage with decreasing i layer thickness, simply because of an increase of the electric field across the i layer.

In the following discussion, we focus only on the thickness independence of the forward current density observed in the linear range (V<0.5 V) of ln(J)-V curves of our p-i-n diodes, because this behavior is quite abnormal from the standpoint of conventional junction theories.

Several theories of crystalline p-i-n diodes are discussed below to clarify

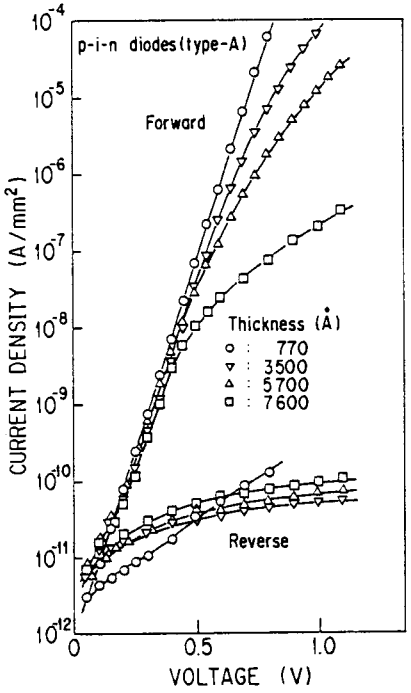

Fig. 10.9. Dependence of J-V characteristics on the thickness of the i layer in p-i-n diodes with SnO_2/ITO/glass substrate (type-A). (After Matsuura *et al.*[19]).

our observations. In the simple theory for crystalline p-i-n diodes,[27] the condition (W=2L_a) gives the transition between short and long p-i-n diodes, where W is the thickness of the i layer and L_a the ambipolar diffusion length. For the long diode structure of W>2L_a, it has been reported in several experiments that the current is proportional to the square of the voltage[28] as predicted by the theoretical consideration.[29] However, our experimental results, shown in Fig. 10.9, differ. For the short diode structure of W<2L_a, the total forward current density J at low voltages is given by a sum of the diffusion component J_{D0} in the neutral regions (both p and n layers) and the bulk recombination component J_{R0} in the i layer;

$$J = J_{D0}[\exp(qV/kT) - 1] + J_{R0}[\exp(qV/2kT) - 1], \tag{24}$$

with

$$J_{D0} = qn_i^2(D_p/L_pN_D + D_n/L_nN_A), \tag{25}$$

and

$$J_{R0} = qn_i W/\tau, \tag{26}$$

where n_i is the intrinsic carrier concentration, D_p and D_n the diffusion coefficients of holes and electrons, respectively, L_p and L_n the diffusion lengths of holes and electrons, respectively, N_D the donor concentration in the n layer, N_A the acceptor concentration in the p layer, τ the carrier lifetime, and W the i layer thickness. The diffusion component J_{D0} does not depend on the i layer thickness, while the bulk recombination component J_{R0} is proportional to the i layer thickness. According to experimental results of crystalline p-i-n diodes,[30,31] the η-value has been known to be 2, i.e., the second term (the bulk recombination component) is considered to predominate in the right-hand side of Eq. (24). From the similar discussion associated with $\eta \sim 2$, Carlson *et al.*[2] and Han *et al.*[7] have suggested that the current transport mechanism, even in a-Si:H p-i-n diodes, is limited by the bulk recombination process, although they have not shown the thickness dependence of J. However, our experimental results of the thickness independence of J_0 is unable to be explained in terms of the bulk recombination regime because J_{R0} should vary with the i layer thickness.

In the early stages of the theoretical investigation of the diode theory, Mott[32] and Schottky[33] presented their original models for the metal-semiconductor junction, taking into account the drift as well as diffusion currents in the depletion layer where the non-negligible effect of carrier collisions is assumed. This assumption is quite plausible in amorphous semiconductors because of the short diffusion length of carriers. In particular, Mott's theory seems to be more suitable for amorphous p-i-n diodes used in this study because the space-charge region is considered to extend over the whole i layer, resulting in a constant electric field across the i layer. This current density, referred to as the diffusion current density, is expressed as

$$J = J_{DD0}[\exp(qV/kT) - 1], \tag{27}$$

where J_{DD0} is a quantity proportional to the constant electric field in the i layer. Chen and Lee[11] numerically analyzed the J-V characteristics of amorphous semiconductor junctions on the basis of the above concepts, and reported that in the case of the diffusion current, the magnitude of the forward current increases with a decrease of the i layer thickness, while the bulk recombination current should increase with the thickness. Therefore, J_{DD0} should change inversely with the i layer thickness, which is, however, not compatible with our experimental results.

Consequently, it is difficult to interpret the present experimental observation on the thickness independence of the junction transport of p-i-n diodes (types A, B, and C) in terms of a bulk effect of the i layer. Some interface or a narrow region, thinner than 770 Å, is considered to limit the junction current in the present p-i-n diodes.

The bulk recombination current expressed by the second term of the right-hand side of Eq. (24) is derived on the assumption that recombination takes place at a maximum rate over the whole i layer region. According to the Shockley-Read-Hall formula, however, the recombination rate takes a maximum value only when the following conditions are satisfied: (1) the hole concentration is equal to the electron concentration and (2) localized states located near the midgap behave as recombination centers. Since the gap states near the midgap of a-Si:H, essentially being dangling bond states, have been known as recombination centers, the recombination current of the p-i-n diode should be limited by the recombination at a narrow zone where condition (1) is satisfied.

The characteristics of the p-i-Mg diodes (type-C) are similar to those of the p-i-n diodes (types A and B), indicating that the n/i interface is not directly associated with the current transport mechanism of the present p-i-n diodes, since Mg forms an ohmic contact with the i layer as well as the n layer.

The above arguments lead us to the conclusion that the p/i interface is one of the most probable candidates for the current-limiting layer. Concerning a possible origin of the interface states at the p/i interface, one is tempted to ascribe one to indium (In) or tin (Sn) atoms which are possibly diffused from SnO_2 or ITO. However, the effect of those atoms on the p/i interface, if such an effect exists, seems to be neglected in the present transport mechanism because the characteristics of the diodes of type-B using a stainless-steel substrate are essentially the same as those of type-A with an SnO_2/ITO/glass substrate.

From the above discussion, it has become clear that the dark forward current of p-i-n diodes must be limited in a narrow region (<770 Å). However, it is still difficult to say where the current is limited.

10.6 Summary

We have investigated various kinds of contacts with amorphous semiconductors and have tried to understand the experimental results using our new models for the junctions of amorphous semiconductors which are characterized as: (1) a much shorter mean-free path of carriers in the extended states, (2) the existence of a lot of gap states, and (3) very high resistivity of films (e.g., 10^9 Ωdm for undoped a-Si:H).

In section 10.2, we have discussed the nature of metal/semiconductor junctions and amorphous/crystalline heterojunctions (metal(Au, Mg)/a-SiH/c-Si(n^+, p^+) diodes) for various doping levels in a-Si:H, and we have

determined the conduction type of a-Si:H in terms of the dominant carrier concentration. The results are as follows.

(1) On the basis of the dominant carrier concentration we have found that P-doped and undoped a-Si:H exhibit n-type, and B-doped a-Si:H exhibits intrinsic and p-type conduction for $B_2H_6/SiH_4 \sim 10^{-6}$ and $>10^{-5}$, respectively;

(2) Mg forms an ohmic contact with undoped and P-doped (i.e., n-type) a-Si:H as well as a-$Si_{1-x}Ge_x$:H, while Au forms an ohmic contact with p-type materials.

In section 10.3, we have investigated amorphous Schottky barrier junctions using several qualities of a-$Si_{1-x}Ge_x$:H materials. Although the η-values were larger than 1.1, the currents were found to be limited by the multistep tunneling process through the Schottky barrier, and not limited by the recombination process in the depletion region. A current peculiar to amorphous Schottky barrier junctions we have proposed as the diffusion-field-emission current, and is expressed as

$$J \propto \exp(V/E_0),$$

with

$$E_0 = E_{00}\coth(qE_{00}/kT)$$

and

$$E_{00} = [(1+\gamma)h/4\pi](N_1/m^*\varepsilon_s)^{1/2},$$

where γ is the multistep tunneling factor. When the density of localized states is considerably high, the forward current becomes the field-emission current given by

$$J \propto \exp(V/E_{00}).$$

When it is fairly low, however, the diffusion current becomes dominant, and is described as

$$J \propto \exp(qV/\eta kT),$$

where $\eta < 1.1$.

In section 10.4, we have presented energy band diagrams for a-Si:H/c-Si heterojunctions on the basis of C-V characteristics of undoped (n-type) a-Si:H heterojunctions formed on p c-Si substrates with four different resistivities. Also we have elucidated the current transport mechanism of

those heterojunction from J-V characteristics and their temperature dependence. The main results are summarized as follows:

(1) The high-frequency (100-kHz) C-V characteristics have been successfully analyzed in the heterojunctions with highly resistive undoped a-Si:H, from which it has been made clear that the abrupt heterojunction model is valid for the a-Si:H/c-Si heterojunctions.

(2) The band off-set in the conduction band and the electron affinity of undoped a-Si:H could be estimated.

(3) The forward current, obtained experimentally as

$$J \propto \exp(-\Delta E_{af}/kT)\exp(AV),$$

can be explained by the multistep tunneling capture-emission model which we have proposed.

In section 10.5, we have investigated the thickness dependence and the temperature dependence of a-Si:H p-i-n diodes, and have discussed the current transport mechanism of the diodes. The main results are as follows.

(1) The forward current of the p-i-n diodes can be limited in a narrow region (<770 Å), such as the p/i interface or a narrow zone of the i layer where the hole concentration is equal to the electron concentration. However, the n/i interface does not play an important role.

(2) Impurities (In and Sn) diffused from SnO_2 and ITO, if they exist, seem to give no fatal influence to the junction properties of p-i-n diodes in the dark.

The formation of ohmic contacts with highly resistive materials is an essential problem when one measures electric properties of the materials. It was found that Mg forms a good ohmic contact with undoped amorphous semiconductors (e.g., a-Si:H and a-$Si_{1-x}Ge_x$:H).[12] After our investigation, Mg has been widely used as an ohmic-contact metal[35-37] and the contact properties have been studied in detail.[38,39]

The study of Schottky barrier junctions could not only lead us to a better understanding of the junction physics of amorphous semiconductors, but also give us a criterion for evaluating the quality of amorphous semiconductors from the viewpoint of devices.

Amorphous/crystalline heterojunctions have recently been applied to solar cells,[40,41] vidicon targets,[42] and bipolar transistors with wide band emitters.[43] Experimental and theoretical investigations of these heterojunctions have also been reported.[44-53] We have recently tried to obtain the density-of-state distribution of undoped amorphous semiconductors using these heterojunctions.[54-57]

The present investigation of p-i-n diodes seems to raise questions as to whether the conventional a-Si:H p-i-n diode theory is valid or not. The answer is not clear at this moment. Much work has to be done in the future.

REFERENCES

1) S. M. Sze: *Physics of Semiconductor Devices,* 2nd ed. (Wiley, New York, 1981).
2) D. E. Carlson and C. R. Wronski: *Appl. Phys. Lett.* **28** (1976) 671.
3) C. R. Wronski, D. E. Carlson, and R. E. Daniel: *Appl. Phys. Lett.* **29** (1976) 602.
4) A. J. Snell, K. D. Mackenzie, P. G. LeComber, and W. E. Spear: *Philos. Mag.* **B40** (1979) 1.
5) R. A. Gibson, P. G. LeComber, and W. E. Spear: *Appl. Phys.* **21** (1980) 307.
6) Y. Mishima, M. Hirose, and Y. Osaka: *Jpn. J. Appl. Phys.* **20** (1981) 593.
7) M. Han, W. A. Anderson, and H. Wiesmann: *16th IEEE Photovoltaic Specialist Conference*, San Diego, 1982, p. 1102.
8) H. Taniguchi, M. Konagai, K. Su Lim, P. Sichanugrist, K. Komori, and K. Takahashi: *Jpn. J. Appl. Phys.* **21**, Suppl. 21-2, (1982) 219.
9) R. J. Nemanich: in *Semiconductors and Semimetals*, edited by J. I. Pankove (Academic Press, Orlando, 1984), Vol. 21, part C, p. 375.
10) W. B. Jackson, R. J. Nemanich, M. J. Thompson, and B. Wacker: *Phys. Rev.* **B33** (1986) 6936.
11) I. Chen and S. Lee: *Proceedings of the 9th International Conference on Amorphous and Liquid Semiconductors*, Grenoble 1981; *J. Phys. (Paris)* **42** (1981) C4-499; *J. Appl. Phys.* **53** (1982) 1045.
12) H. Matsuura, T. Okuno, H. Okushi, S. Yamasaki, A. Matsuda, N. Hata, H. Oheda, and K. Tanaka: *Jpn. J. Appl. Phys.* **22** (1983) L197.
13) H. Matsuura, A. Matsuda, H. Okushi, T. Okuno, and K. Tanaka: *Appl. Phys. Lett.* **45** (1984) 433.
14) H. Matsuura and H. Okushi: *J. Appl. Phys.* **62** (1987) 2871.
15) V. Šmíd, J. J. Mares, L. Štourač, and J. Krištofik: *Tetrahedrally-Bonded Amorphous Semiconductors,* edited by D. Adler and H. Fritzsche (Plenum, New York, 1985), p. 483.
16) H. Matsuura, H. Okushi, and K. Tanaka: *Proceedings of the 12th International Conference on Amorphous and Liquid Semiconductors*, Prague 1987; *J. Non-Cryst. Solids* **97/98** (1987) 963.
17) S. M. Sze: *Physics of Semiconductor Devices*, 2nd ed. (Wiley, New York, 1981), p. 254.
18) F. A. Padovani and R. Stratton: *Solid State Electron.* **9** (1966) 695.
19) H. Matsuura, A. Matsuda, H. Okushi, and K. Tanaka: *J. Appl. Phys.* **58** (1985) 1578.
20) H. Matsuura, T. Okuno, H. Okushi, N. Hata, S. Yamasaki, H. Oheda, A. Matsuda, and K. Tanaka: *Extended Abstracts of the 15th Conference on Solid State Devices and Materials*, Tokyo 1983, p. 185.
21) H. Matsuura, T. Okuno, H. Okushi, and K. Tanaka: *J. Appl. Phys.* **55** (1984) 1012.
22) H. Matsuura: *Jpn. J. Appl. Phys.* **27** (1988) L513.
23) J. D. Cohen and D. V. Lang: *Phys. Rev.* **B25** (1982) 5321.
24) S. M. Sze: *Physics of Semiconductor Devices*, 2nd ed. (Wiley, New York, 1981), p. 275.
25) A. R. Riben and D. L. Feucht: *Solid-State Electron.* **9** (1966) 1055.
26) A. G. Chynoweth, W. L. Feldmann, and R. A. Logan: *Phys. Rev.* **121** (1961) 684.
27) S. M. Sze: *Physics of Semiconductor Devices*, 2nd ed. (Wiley, New York, 1981), p. 120.
28) R. D. Larrabee: *Phys. Rev.* **121** (1961) 37.
29) M. A. Lampert and A. Rose: *Phys. Rev.* **121** (1961) 26.
30) R. N. Hall: *Proc. IRE* **40** (1952) 1512.
31) H. S. Veloric and M. B. Prince: *Bell syst. Tech. J.* **36** (1957) 975.
32) N. F. Mott: *Proc. R. Soc.* **171** (1932) 27.
33) W. Schottky: *Z. Phys.* **113** (1931) 367.
34) A. S. Grove: *Physics and Technology of Semiconductor Devices* (Wiley, New York, 1967), p. 186.

35) K. Shimakawa and Y. Yano: *Appl. Phys. Lett.* **45** (1984) 862.
36) H. Oheda: *Philos. Mag.* **B52** (1985) 857.
37) K. Shimakawa and Y. Katsuma: *J. Appl. Phys.* **60** (1986) 1417.
38) J. Kanicki, M. O. Aboelfotoh, and W. Bauhofer: *Proceedings of the 17th International Conference on Physics of Semiconductors*, edited by J. D. Chadi and W. A. Harrison (Springer, New York, 1985), p. 183.
39) J. Kanicki and D. Bullock: *Mater. Res. Soc. Symp. Proc.* **70** (1986) 379.
40) K. Okuda, H. Okamoto and Y. Hamakawa, *Jpn. J. Appl. Phys.* **22** (1983) L605.
41) M. M. Rahman and S. Furukawa: *Jpn. J. Appl. Phys.* **23** (1984) 515.
42) H. Mimura and Y. Hatanaka: *Extended Abstracts of the 17th Conference on Solid State Devices and Materials,* Tokyo 1985, p. 115.
43) K. Sasaki, S. Furukawa, and M. M. Rahman: *Extended Abstracts of the 17th Conference on Solid State Devices and Materials,* Tokyo 1985, p. 385.
44) H. Mimura and Y. Hatanaka: *Appl. Phys. Lett.* **45** (1984) 452.
45) H. Mimura and Y. Hatanaka: *Jpn. J. Appl. Phys.* **24** (1985) L355.
46) H. Mimura and Y. Hatanaka: *Jpn. J. Appl. Phys.* **26** (1987) 60.
47) H. Mimura and Y. Hatanaka: *J. Appl. Phys.* **61** (1987) 2575.
48) H. Mimura and Y. Hatanaka: *Appl. Phys. Lett.* **50** (1987) 326.
49) F. A. Rubinelli, S. Albornoz, and R. H. Buitrago: *Technical Digest of the 1st International Photovoltaic Science and Engineering Conference*, Kobe 1984, p. 115.
50) F. A. Rubinelli, M. R. Battioni, and R. H. Buitrago: *J. Appl. Phys.* **61** (1987) 650.
51) F. A. Rubinelli, S. Albornoz, and R. H. Buitrago: *Solid-State Electron.* **28** (1985) 741.
52) Z. Y. Xu, W. Chen, B. F. Zhao, C. A. Wang, F. Q. Zhang, and J. Y. Wang: *Proceedings of the 12th International Conference on Amorphous and Liquid Semiconductors,* Prague 1987; *J. Non-Crys. Solids* **97/98** (1987) 983.
53) W. Wang and K. Liao: *Mater. Res. Soc. Symp. Proc.* **70** (1986) 399.
54) H. Matsuura: *Jpn. J. Appl. Phys.* **27** (1988) L516.
55) H. Matsuura: *J. Appl. Phys.* **64** (1988) 1964.
56) H. Matsuura: *Appl. Phys. Lett.* **54** (1989) 344.
57) H. Matsuura, Z E. Smith, A. Matsuda, S. Yokoyama, M. Tanaka, M. Ueda, and K. Tanaka: *Phil. Mag. Lett.* **59** (1989) 109.